Interaction of newly defined stress intensity factors for angular corners in two diamond-shaped inclusions

N.-A. Noda,[a] K. Oda,[b] Y.Kawashima[a]
[a]*Department of Mechanical Engineering, Kyushu Institute of Technology, 1-1 Sensuicho, Tobata-ku, Kitayushu 804, Japan*
[b]*Department of Mechanical & Electrical Engineering, Tokuyama College of Technology, 3538 Takajo, Kume, Tokuyama 745, Japan*

Abstract

This paper deals with numerical solutions of singular integral equations in interaction problems of diamond-shaped inclusions with angular corners under various loading conditions. The problems are formulated as a system of singular integral equations with Cauchy-type or logarithmic-type singularities, where the unknown functions are the densities of body forces distributed in infinite plates having the same elastic constants of the matrix and inclusions. In order to analyze the problems accurately, the unknown functions of the body force densities are expressed as a linear combination of two types of fundamental density functions and power series, where the fundamental density functions are chosen to represent the symmetric stress singularity of $1/r^{1-\lambda 1}$ and the skew-symmetric stress singularity of $1/r^{1-\lambda 2}$. Then, newly defined stress intensity factors of angular corners are systematically calculated for various shapes and spacing of two diamond-shaped inclusions in a plate subjected to uniaxial tension, biaxial tension and in-plane shear. The present method is found to yield rapidly conversing numerical results for interaction of diamond-shaped inclusions.

1 Introduction

In the evaluation of interface strength in composites and bonded materials, it is necessary to know the singular stress field at the angular corner in dissimilar materials accurately. Hence, problems of stress singularity at the angular corner have been treated in many papers.[1-7, 11-13] In this problem, differing from the crack problem having the stress singularity of $1/r^{1/2}$, there appear two types of

stress singularities $1/r^{1-\lambda 1}$ and $1/r^{1-\lambda 2}$, where $1-\lambda_1$ and $1-\lambda_2$ are the orders of singularity of stress field for the mode I and mode II deformation, respectively. Recently, Chen & Nisitani [4, 5] have pointed out that the singular stress field near an angular corner is defined in terms of four parameters, that is, λ_1, λ_2 and K_{I,λ_1}, K_{II,λ_2}, as follows.

$$\sigma_{ij} = \frac{K_{I,\lambda_1}}{r^{1-\lambda_1}} f_{ij}^{I}(\theta) + \frac{K_{II,\lambda_2}}{r^{1-\lambda_2}} f_{ij}^{II}(\theta) \tag{1}$$

In eqn (1), K_{I,λ_1} and K_{II,λ_2} are the parameters which express the intensities of singular stress field near an angular corner in a similar way of the stress intensity factor in ordinary cracks. In many studies on the singular stress at the angular corner, however, two types of singular stresses have not been taken into account sufficiently.[3-5]

In this paper, the interaction problem of two diamond-shaped inclusions in an infinite plate is analyzed as illustrated in Fig. 1. The newly defined stress intensity factors of the angular corners are systematically calculated for various geometrical and loading conditions and interaction effect of angular corners is considered. In this analysis, numerical solution of singular integral equation of the body force method is considered,[8-11] where unknown functions are approximated by the products of fundamental density functions and polynomials. In our previous papers,[8-11] the numerical method has been found to yield rapidly conversing the results with high accuracy. The diamond-shaped inclusion can be regarded as a basic model of inclusion with the angular corners and the results can be applied to estimate the stress intensity factors for a polygonal inclusion with the same angle of the corner and the same projected length of inclusion in a direction perpendicular to the tensile axis.[6, 7] In this study, three fundamental types of loading conditions, (i) uniaxial tension, (ii) biaxial tension and (iii) in-plane shear are treated.

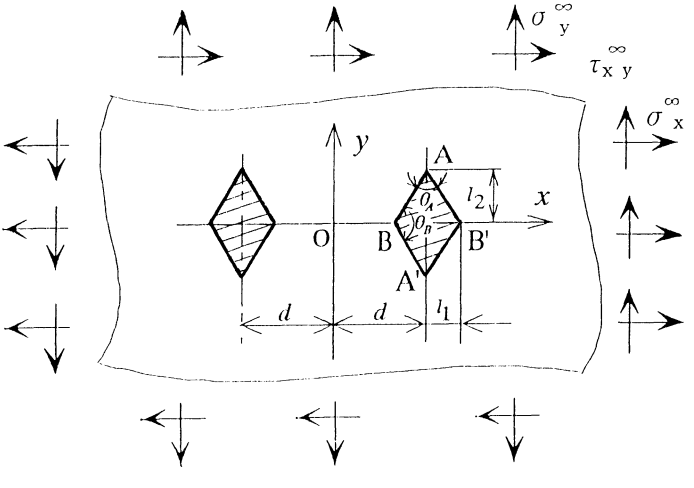

Figure 1: Two diamond-shaped inclusions in an infinite plate.

2 Numerical solution of singular integral equation in interaction problem of angular corners

Consider two diamond-shaped inclusions with the same size in an infinite plate subjected to the stresses σ_x^∞, σ_y^∞ and τ_{xy}^∞ at infinity as shown in Fig.1. The shear modulus and Poisson's ratios of the matrix and the inclusion are to be (G_1, ν_1) and (G_2, ν_2), respectively.

In this analysis, the problem is expressed as a linear combination of two types of body forces distributed along the imaginary boundary in two infinite plates (infinite plate M and infinite plate I). Here, the infinite plate 'M' and the infinite plate 'I' have the same elastic constants of the matrix (G_1, ν_1) and the inclusions (G_2, ν_2), respectively. In order to express the mode I and the mode II deformation at the inclusion corner, two types of pairs of body forces, that is, a symmetric type (mode I) and a skew-symmetric type (mode II) to the bisector of the corner, are distributed normal (θ-direction) and tangential (r-direction) to the prospective boundary of the inclusion.[11, 12] Since the orders of stress singularity are different between at the corners A and B, the side $\overline{AB}$ is divided into two equal parts for the convenience of numerical analysis. These body forces are to be distributed around the corners A, A', B, B' and imaginary boundaries with respect to y-axis in a similar manner. The boundary conditions of stress and displacement are satisfied by applying the linear combination of these body forces. Based on the idea of the body force method mentioned above, the singular integral equations are expressed as follows, where the body force densities distributed along the prospective boundary of the diamond-shaped inclusions in the infinite plates M and I in θ- and r-directions, $F_{\theta M}(r)$, $F_{rM}(r)$ $F_{\theta I}(r)$, $F_{rI}(r)$, are to be unknown functions.

$$
\begin{aligned}
&-\frac{1}{2}F_{\theta M}(s)+\frac{1}{2}F_{\theta I}(s)+\int_0^{l_{AB}/2}h_{nnM}^{F_\theta}(r_A,s)F_{\theta AM}(r_A)dr_A+\int_0^{l_{AB}/2}h_{nnM}^{F_r}(r_A,s)F_{rAM}(r_A)dr_A\\
&\quad+\int_0^{l_{AB}/2}h_{nnM}^{F_\theta}(r_{A'},s)F_{\theta A'M}(r_{A'})dr_{A'}+\int_0^{l_{AB}/2}h_{nnM}^{F_\theta}(r_{A'},s)F_{rA'M}(r_{A'})dr_{A'}\\
&\quad+\int_0^{l_{AB}/2}h_{nnM}^{F_\theta}(r_B,s)F_{\theta BM}(r_B)dr_B+\int_0^{l_{AB}/2}h_{nnM}^{F_r}(r_B,s)F_{rBM}(r_B)dr_B\\
&\quad+\int_0^{l_{AB}/2}h_{nnM}^{F_\theta}(r_{B'},s)F_{\theta A'M}(r_{B'})dr_{B'}+\int_0^{l_{AB}/2}h_{nnM}^{F_\theta}(r_{B'},s)F_{rB'M}(r_{B'})dr_{B'}\\
&\quad-\int_0^{l_{AB}/2}h_{nnI}^{F_\theta}(r_A,s)F_{\theta AI}(r_A)dr_A-\int_0^{l_{AB}/2}h_{nnI}^{F_r}(r_A,s)F_{rAI}(r_A)dr_A\\
&\quad-\int_0^{l_{AB}/2}h_{nnI}^{F_\theta}(r_{A'},s)F_{\theta A'I}(r_{A'})dr_{A'}-\int_0^{l_{AB}/2}h_{nnI}^{F_\theta}(r_{A'},s)F_{rA'I}(r_{A'})dr_{A'}\\
&\quad-\int_0^{l_{AB}/2}h_{nnI}^{F_\theta}(r_B,s)F_{\theta BI}(r_B)dr_B-\int_0^{l_{AB}/2}h_{nnI}^{F_r}(r_B,s)F_{rBI}(r_B)dr_B\\
&\quad-\int_0^{l_{AB}/2}h_{nnI}^{F_\theta}(r_{B'},s)F_{\theta A'I}(r_{B'})dr_{B'}-\int_0^{l_{AB}/2}h_{nnI}^{F_\theta}(r_{B'},s)F_{rB'I}(r_{B'})dr_{B'}=-\sigma_{nM}^\infty(s)+\sigma_{nI}^\infty(s)
\end{aligned}
$$

$$
\begin{aligned}
&-\frac{1}{2}F_{rM}(s)+\frac{1}{2}F_{rI}(s)+\int_0^{l_{AB}/2}h^{F_\theta}_{tnM}(r_A,s)F_{\theta AM}(r_A)dr_A+\int_0^{l_{AB}/2}h^{F_r}_{ntM}(r_A,s)F_{rAM}(r_A)dr_A\\
&\quad+\int_0^{l_{AB}/2}h^{F_\theta}_{ntM}(r_{A'},s)F_{\theta A'M}(r_{A'})dr_{A'}+\int_0^{l_{AB}/2}h^{F_\theta}_{ntM}(r_{A'},s)F_{rA'M}(r_{A'})dr_{A'}\\
&\quad+\int_0^{l_{AB}/2}h^{F_\theta}_{ntM}(r_B,s)F_{\theta BM}(r_B)dr_B+\int_0^{l_{AB}/2}h^{F_r}_{ntM}(r_B,s)F_{rBM}(r_B)dr_B\\
&\quad+\int_0^{l_{AB}/2}h^{F_\theta}_{ntM}(r_{B'},s)F_{\theta A'M}(r_{B'})dr_{B'}+\int_0^{l_{AB}/2}h^{F_\theta}_{ntM}(r_{B'},s)F_{rB'M}(r_{B'})dr_{B'}\\
&\quad-\int_0^{l_{AB}/2}h^{F_\theta}_{ntI}(r_A,s)F_{\theta AI}(r_A)dr_A-\int_0^{l_{AB}/2}h^{F_r}_{ntI}(r_A,s)F_{rAI}(r_A)dr_A\\
&\quad-\int_0^{l_{AB}/2}h^{F_\theta}_{ntI}(r_{A'},s)F_{\theta A'I}(r_{A'})dr_{A'}-\int_0^{l_{AB}/2}h^{F_\theta}_{ntI}(r_{A'},s)F_{rA'I}(r_{A'})dr_{A'}\\
&\quad-\int_0^{l_{AB}/2}h^{F_\theta}_{ntI}(r_B,s)F_{\theta BI}(r_B)dr_B-\int_0^{l_{AB}/2}h^{F_r}_{ntI}(r_B,s)F_{rBI}(r_B)dr_B\\
&\quad-\int_0^{l_{AB}/2}h^{F_\theta}_{ntI}(r_{B'},s)F_{\theta A'I}(r_{B'})dr_{B'}-\int_0^{l_{AB}/2}h^{F_\theta}_{ntI}(r_{B'},s)F_{rB'I}(r_{B'})dr_{B'}=-\tau^{\infty}_{ntM}(s)+\tau^{\infty}_{ntI}(s)
\end{aligned}
\tag{2}
$$

$$
\begin{aligned}
&\int_0^{l_{AB}/2}h^{F_\theta}_{uM}(r_A,s)F_{\theta AM}(r_A)dr_A+\int_0^{l_{AB}/2}h^{F_r}_{uM}(r_A,s)F_{rAM}(r_A)dr_A+\int_0^{l_{AB}/2}h^{F_\theta}_{uM}(r_{A'},s)F_{\theta A'M}(r_{A'})dr_{A'}\\
&+\int_0^{l_{AB}/2}h^{F_\theta}_{uM}(r_{A'},s)F_{rA'M}(r_{A'})dr_{A'}+\int_0^{l_{AB}/2}h^{F_\theta}_{uM}(r_B,s)F_{\theta BM}(r_B)dr_B+\int_0^{l_{AB}/2}h^{F_r}_{uM}(r_B,s)F_{rBM}(r_B)dr_B\\
&+\int_0^{l_{AB}/2}h^{F_\theta}_{uM}(r_{B'},s)F_{\theta A'M}(r_{B'})dr_{B'}+\int_0^{l_{AB}/2}h^{F_\theta}_{uM}(r_{B'},s)F_{rB'M}(r_{B'})dr_{B'}\\
&-\int_0^{l_{AB}/2}h^{F_\theta}_{ul}(r_A,s)F_{\theta AI}(r_A)dr_A-\int_0^{l_{AB}/2}h^{F_r}_{ul}(r_A,s)F_{rAI}(r_A)dr_A-\int_0^{l_{AB}/2}h^{F_\theta}_{ul}(r_{A'},s)F_{\theta A'I}(r_{A'})dr_{A'}\\
&-\int_0^{l_{AB}/2}h^{F_\theta}_{ul}(r_{A'},s)F_{rA'I}(r_{A'})dr_{A'}-\int_0^{l_{AB}/2}h^{F_\theta}_{ul}(r_B,s)F_{\theta BI}(r_B)dr_B-\int_0^{l_{AB}/2}h^{F_r}_{ul}(r_B,s)F_{rBI}(r_B)dr_B\\
&-\int_0^{l_{AB}/2}h^{F_\theta}_{ul}(r_{B'},s)F_{\theta A'I}(r_{B'})dr_{B'}-\int_0^{l_{AB}/2}h^{F_\theta}_{ul}(r_{B'},s)F_{rB'I}(r_{B'})dr_{B'}=-U^{\infty}_{M}(s)+U^{\infty}_{I}(s)
\end{aligned}
$$

$$
\begin{aligned}
&\int_0^{l_{AB}/2}h^{F_\theta}_{vM}(r_A,s)F_{\theta AM}(r_A)dr_A+\int_0^{l_{AB}/2}h^{F_r}_{vM}(r_A,s)F_{rAM}(r_A)dr_A+\int_0^{l_{AB}/2}h^{F_\theta}_{vM}(r_{A'},s)F_{\theta A'M}(r_{A'})dr_{A'}\\
&+\int_0^{l_{AB}/2}h^{F_\theta}_{vM}(r_{A'},s)F_{rA'M}(r_{A'})dr_{A'}+\int_0^{l_{AB}/2}h^{F_\theta}_{vM}(r_B,s)F_{\theta BM}(r_B)dr_B+\int_0^{l_{AB}/2}h^{F_r}_{vM}(r_B,s)F_{rBM}(r_B)dr_B\\
&+\int_0^{l_{AB}/2}h^{F_\theta}_{vM}(r_{B'},s)F_{\theta A'M}(r_{B'})dr_{B'}+\int_0^{l_{AB}/2}h^{F_\theta}_{vM}(r_{B'},s)F_{rB'M}(r_{B'})dr_{B'}\\
&-\int_0^{l_{AB}/2}h^{F_\theta}_{vI}(r_A,s)F_{\theta AI}(r_A)dr_A-\int_0^{l_{AB}/2}h^{F_r}_{vI}(r_A,s)F_{rAI}(r_A)dr_A-\int_0^{l_{AB}/2}h^{F_\theta}_{vI}(r_{A'},s)F_{\theta A'I}(r_{A'})dr_{A'}\\
&-\int_0^{l_{AB}/2}h^{F_\theta}_{vI}(r_{A'},s)F_{rA'I}(r_{A'})dr_{A'}-\int_0^{l_{AB}/2}h^{F_\theta}_{vI}(r_B,s)F_{\theta BI}(r_B)dr_B-\int_0^{l_{AB}/2}h^{F_r}_{vI}(r_B,s)F_{rBI}(r_B)dr_B\\
&-\int_0^{l_{AB}/2}h^{F_\theta}_{vI}(r_{B'},s)F_{\theta A'I}(r_{B'})dr_{B'}-\int_0^{l_{AB}/2}h^{F_\theta}_{vI}(r_{B'},s)F_{rB'I}(r_{B'})dr_{B'}=-V^{\infty}_{M}(s)+V^{\infty}_{I}(s)
\end{aligned}
\tag{3}
$$

In eqns (2) and (3), l_{AB} is the length of side $\overline{AB}$ and $\sigma^{\infty}_{nM}(s)$, $\tau^{\infty}_{ntM}(s)$ (or $\sigma^{\infty}_{nI}(s)$, $\tau^{\infty}_{ntI}(s)$) and $U^{\infty}_{M}(s)$, $V^{\infty}_{M}(s)$ (or $U^{\infty}_{I}(s)$, $V^{\infty}_{I}(s)$) are the stress and displacement, respectively, due to the stress at infinity. Taking $h^{F_\theta}_{nnM}(r_A,s)$ for example, the notation means the normal stress σ_n induced at the collocation point 's' on the imaginary boundary in the infinite plate M when the point forces (symmetric and skew-symmetric type) with unit density in the θ-direction are acting at the point

'r_A' on the imaginary boundary in the infinite plate M, where 's' and 'r_A' are distances measured from the corner A. The equations (2) and (3) are virtually the boundary conditions at the connecting boundary of matrix and inclusion; that is, $\sigma_{nM} - \sigma_{nI} = 0$, $\tau_{ntM} - \tau_{ntI} = 0$, $U_M - U_{tI} = 0$ and $V_M - V_{tI} = 0$. Here, σ_{nM}, τ_{ntM}, U_M and V_M denote the stress and displacement on the imaginary boundary in the infinite plate M and σ_{nI}, τ_{ntI}, U_I and V_I denote the stress and displacement on the imaginary boundary of the inclusion in the infinite plate I. The boundary integral equations corresponding to other corners are also expressed in a similar way.

In this study, the unknown functions of the body force densities $F_{\theta AM}$, F_{rAM}, $F_{\theta AI}$ and F_{rAI} are approximated by a linear combination of weight functions ($W^I_{\theta AM} \sim W^{II}_{rAI}$) and two types of fundamental density functions.[11]

$$
\begin{aligned}
F_{\theta AM}(r_A) &= F^I_{\theta AM}(r_A) + F^{II}_{\theta AM}(r_A) = W^I_{\theta AM}(r_A) r_A^{\lambda_1 - 1} + W^{II}_{\theta AM}(r_A) r_A^{\lambda_2 - 1} \\
F_{rAM}(r_A) &= F^I_{rAM}(r_A) + F^{II}_{rAM}(r_A) = W^I_{rAM}(r_A) r_A^{\lambda_1 - 1} + W^{II}_{rAM}(r_A) r_A^{\lambda_2 - 1} \\
F_{\theta AI}(r_A) &= F^I_{\theta AI}(r_A) + F^{II}_{\theta AI}(r_A) = W^I_{\theta AI}(r_A) r_A^{\lambda_1 - 1} + W^{II}_{\theta AI}(r_A) r_A^{\lambda_2 - 1} \\
F_{rAI}(r_A) &= F^I_{rAI}(r_A) + F^{II}_{rAI}(r_A) = W^I_{rAI}(r_A) r_A^{\lambda_1 - 1} + W^{II}_{rAI}(r_A) r_A^{\lambda_2 - 1}
\end{aligned} \tag{4}
$$

$$
\begin{aligned}
&W^I_{\theta AM}(r_A) = \sum_{n=1}^{N} a_n r_A^{n-1},\ W^I_{rAM}(r_A) = \sum_{n=1}^{N} b_n r_A^{n-1},\ W^{II}_{\theta AM}(r_A) = \sum_{n=1}^{N} c_n r_A^{n-1},\ W^{II}_{rAM}(r_A) = \sum_{n=1}^{N} d_n r_A^{n-1} \\
&W^I_{\theta AI}(r_A) = \sum_{n=1}^{N} e_n r_A^{n-1},\ W^I_{rAI}(r_A) = \sum_{n=1}^{N} f_n r_A^{n-1},\ W^{II}_{\theta AI}(r_A) = \sum_{n=1}^{N} g_n r_A^{n-1},\ W^{II}_{rAI}(r_A) = \sum_{n=1}^{N} h_n r_A^{n-1}
\end{aligned} \tag{5}
$$

Here, $r_A^{\lambda_1 - 1}$ and $r_A^{\lambda_2 - 1}$ are the fundamental density functions to express the stress singularities of mode I and mode II at the angular corner A, respectively.[11, 12] The eigenvalues of λ_1 and λ_2 are given as the roots of the eigenequations, which are related only to the material combination and the vertex angle of corner.[4,5] The superscripts I and II mean the distribution types of body force, that is, symmetrical (mode I) and skew-symmetrical (mode II) to the bisector of the corner, respectively.

By using the numerical method mentioned above, the integral equations (2) and (3) are solved and the unknown coefficients $a_n \sim h_n$ are determined from the boundary conditions at the collocation points on the imaginary boundary. The stress intensity factors K_{I,λ_1} and K_{II,λ_2} at the inclusion corner A defined by eqn (1) can be obtained from the values of weight functions at the corner tip as follows.[7, 12]

$$
K_{I,\lambda_1} = \frac{1}{\lambda_1} \times \frac{-2\sqrt{2\pi}(\alpha - \beta)(\kappa_1 q_7 + \lambda_1 q_1)}{2[\{\lambda_1(\alpha - \beta)q_4 + (1 - \beta)q_2\}p_5 + \{(\lambda_1 + 1)(\alpha - \beta)q_3\}p_6](\kappa_1 q_7 + \lambda_1 q_1)}
$$

$$
-[\{\lambda_1(\alpha - \beta)q_4 + (1 - \beta)q_2\}p_5 + \{(\lambda_1 - \kappa_1)(\alpha - \beta)q_3\}p_6]\{(\kappa_1 - 1)q_7 + (\kappa_1 + 2\lambda_1 + 1)q_1\}
$$

$$
+[\{\lambda_1(\alpha - \beta)q_4 + (1 - \beta)q_2\}q_5 + \{(\lambda_1 + \kappa_1)(\alpha - \beta)q_3\}q_6](\kappa_1 + 1)(p_1 + p_7) \times W^I_{\theta AM}(0)
$$

$$p_1 = \cos\gamma,\quad p_2 = \cos(\lambda_1\pi),\quad p_3 = \cos\{\lambda_1(\gamma-\pi)\},\quad p_4 = \cos\{\gamma-\lambda_1(\gamma-\pi)\}$$
$$p_5 = \cos\{(\lambda_1+1)\gamma/2\},\quad p_6 = \cos\{(\lambda_1-1)\gamma/2\},\quad p_7 = \cos(2\lambda_1\pi-\lambda_1\gamma)$$
$$q_1 = \sin\gamma,\quad q_2 = \sin(\lambda_1\pi),\quad q_3 = \sin\{\lambda_1(\gamma-\pi)\},\quad q_4 = \sin\{\gamma-\lambda_1(\gamma-\pi)\}$$
$$q_5 = \sin\{(\lambda_1+1)\gamma/2\},\quad q_6 = \sin\{(\lambda_1-1)\gamma/2\},\quad q_7 = \sin(2\lambda_1\pi-\lambda_1\gamma)$$
$$\gamma = 2\pi-\theta_A \tag{6}$$

$$K_{II,\lambda_2} = \frac{1}{\lambda_2}\times\frac{2\sqrt{2\pi}(\alpha-\beta)(\kappa_1 q_{13}-\lambda_2 q_1)}{2[\{\lambda_2(\alpha-\beta)q_{10}-(1-\beta)q_8\}q_{11}+\{(\lambda_2+1)(\alpha-\beta)q_9\}q_{12}](\kappa_1 q_{13}-\lambda_2 q_1)}$$
$$-[\{\lambda_2(\alpha-\beta)q_{10}-(1-\beta)q_8\}q_{11}+\{(\lambda_2-\kappa_1)(\alpha-\beta)q_9\}q_{12}]\{(1-\kappa_1)q_{13}+(\kappa_1+2\lambda_2+1)q_1\}$$
$$+[\{\lambda_2(\alpha-\beta)q_{10}-(1-\beta)q_8\}p_{11}+\{(\lambda_2+\kappa_1)(\alpha-\beta)q_9\}p_{12}](\kappa_1+1)(p_{13}-p_1)\times W^{II}_{\theta AM}(0)$$

$$p_1 = \cos\gamma,\quad p_8 = \cos(\lambda_2\pi),\quad p_9 = \cos\{\lambda_2(\gamma-\pi)\},\quad p_{10} = \cos\{\gamma-\lambda_2(\gamma-\pi)\}$$
$$p_{11} = \cos\{(\lambda_2+1)\gamma/2\},\quad p_{12} = \cos\{(\lambda_2-1)\gamma/2\},\quad p_{13} = \cos(2\lambda_2\pi-\lambda_2\gamma)$$
$$q_1 = \sin\gamma,\quad q_8 = \sin(\lambda_2\pi),\quad q_9 = \sin\{\lambda_2(\gamma-\pi)\},\quad q_{10} = \sin\{\gamma-\lambda_2(\gamma-\pi)\}$$
$$q_{11} = \sin\{(\lambda_2+1)\gamma/2\},\quad q_{12} = \sin\{(\lambda_2-1)\gamma/2\},\quad q_{13} = \sin(2\lambda_2\pi-\lambda_2\gamma)$$
$$\gamma = 2\pi-\theta_A \tag{7}$$

In eqns (6) and (7), α and β are Dunders' composite parameters,[1] and κ_1=3–4ν_1 (plane strain) or =(3–ν_1)/(1+ν_1) (plane stress). The similar relations $K_{I,\lambda_1} - W^{I}_{rAM}(0)$ and $K_{II,\lambda_2} - W^{II}_{rAM}(0)$ cannot be shown here for lack of space.

3 Results and discussion

The interaction problem of two diamond-shaped inclusions is analyzed under three fundamental loads, uniaxial tension, biaxial tension and in-plane shear.

First, the accuracy of the present method for this problem is examined. As mentioned in Section 2, the both values of K_{I,λ_1} (or K_{II,λ_2}) obtained from values of weight functions in θ- and r-directions at the corner tip should be in agreement with each other within the error of numerical calculation. As an example, the convergency of the numerical results with increasing the number of collocation points N is shown in Table 1 when $\theta_A = 60°$, $\nu_1 = \nu_2 = 0.3$, $l_2/d = 1/2$, $G_2/G_1 = 0.1$, $\sigma^\infty_x = \sigma^\infty_y = \sigma^\infty$ and $\tau^\infty_{xy} = 0$. The obtained results are written by the following dimensionless expressions:

$$F_{I,\lambda_1} = K_{I,\lambda_1}\Big/\sigma^\infty\sqrt{\pi}\,l_2^{1-\lambda_1},\quad F_{II,\lambda_2} = K_{II,\lambda_2}\Big/\sigma^\infty\sqrt{\pi}\,l_2^{1-\lambda_2} \tag{8}$$

In Table 1, the notation N is the number of collocation points near the corner A and the total number of collocation points is 8N. The unknown coefficients in the weight functions (5) are determined by solving the 32N algebraic equations. The numerical results obtained from the values of weight functions in θ- and r-directions coincide with each other in about four digits when N=12 and it is

Table 1: Convergency of F_{I,λ_1} and F_{II,λ_2} at the corner A ($\theta_A = 60°$, $l_2/d = 1/2$, $G_2/G_1 = 10^{-1}$, $\sigma_x^\infty = \sigma_y^\infty = \sigma^\infty$, $\tau_{xy}^\infty = 0$, $\nu_1 = \nu_2 = 0.3$ and plane strain state in Fig.1)

	F_{I,λ_1} (λ_1=0.6900333)		F_{II,λ_2} (λ_2=0.7940938)	
N	from $W_r^I(0)$	from $W_r^{II}(0)$	from $W_r^I(0)$	from $W_r^{II}(0)$
4	0.62575	0.62558	0.01699	0.01699
6	0.62611	0.62599	0.01701	0.01701
8	0.62622	0.62614	0.01702	0.01702
10	0.62626	0.62621	0.01703	0.01703
12	0.62627	0.62623	0.01704	0.01705

found that the present method has good convergency. For various geometrical conditions, it is confirmed that the present method yields rapidly conversing numerical results and is useful for analyzing this problem.

Next, the stress intensity factors of two diamond-shaped inclusions are calculated when the size, the spacing and the elastic constant of inclusions are changed systematically. As an example, Table 2 and 3 show the dimensionless factors F_{I,λ_1} and F_{II,λ_2} at the corners B and B' ($\theta_B \leq 90°$) under uniaxial tension and in-plane shear, respectively. They are calculated under plane strain state (ν_1= ν_2=0.3). When $l_1/d = 0$, the results of $G_2/G_1 = 10^{-5}$ and $G_2/G_1 = 10^5$ correspond to the results of the single diamond-shaped hole and the single diamond-shaped rigid inclusion in an infinite plate, respectively. The present results coincide completely with the results given by Chen & Nisitani [6, 7] in about 4 digits. In Table 2, when $\theta_B = 90°$, $l_1/d = 2/3$ and $G_2/G_1 > 1$, the interaction effect appears largely and F_{I,λ_1} increases by about 50 percent. In Table 3, when $\theta_B = 90°$, $l_1/d = 2/3$ and $G_2/G_1 < 1$, F_{II,λ_2} also increases by about 40 percent. In this case, the values of F_{II,λ_2} themselves are also very large. From the results of various geometrical and loading conditions, the interaction effect of two diamond-shaped inclusions is not very large in most cases and variation of stress intensity factor is within about 20 percent in the range of $l_1/d \leq 2/3$ or $l_2/d \leq 2/3$ except for two cases mentioned above.

4 Conclusion

This paper dealt with the analysis of the interaction problem of two diamond-shaped inclusions with the same size. The newly defined stress intensity factors of the inclusion corner were calculated very accurately by using the singular integral equations of the body force method. The interaction effect of the angular corners was also discussed under various geometrical and loading conditions. The conclusions can be made as follows.

(1) In the numerical solution of the singular integral equations of the body force method, the unknown functions were approximated by the products of the

Table 2: F_{I,λ_1} for two diamond-shaped inclusions at the corners B and B' under uniaxial tension (Plane strain state, $\nu_1 = \nu_2 = 0.3$).

Uniaxial tension: F_{I,λ_1}

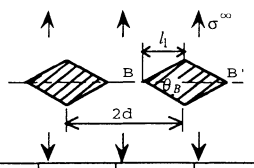

$\left(F_{I,\lambda_1} = K_{I,\lambda_1} / \sigma^{\infty} \sqrt{\pi} l_1^{1-\lambda_1}\right)$

θ_B	l_1/d		G_2/G_1 10^{-5}	10^{-2}	10^{-1}	10^{1}	10^{2}	10^{5}
30°	0	B,B'	1.042	0.909	0.747	-0.160	-0.174	-0.177
	1/3	B	1.062	0.925	0.755	-0.165	-0.179	-0.184
		B'	1.057	0.921	0.754	-0.164	-0.178	-0.181
	1/2	B	1.092	0.947	0.764	-0.169	-0.185	-0.193
		B'	1.072	0.932	0.757	-0.166	-0.180	-0.183
	2/3	B	1.156	0.996	0.783	-0.179	-0.199	-0.204
		B'	1.096	0.948	0.761	-0.168	-0.184	-0.189
60°	0	B,B'	1.148	1.054	0.717	-0.154	-0.173	-0.175
	1/3	B	1.164	1.068	0.722	-0.154	-0.175	-0.178
		B'	1.160	1.065	0.721	-0.152	-0.172	-0.175
	1/2	B	1.190	1.090	0.731	-0.162	-0.185	-0.187
		B'	1.174	1.076	0.725	-0.155	-0.176	-0.181
	2/3	B	1.252	1.143	0.753	-0.178	-0.206	-0.208
		B'	1.197	1.095	0.730	-0.159	-0.181	-0.186
90°	0	B,B'	1.293	1.223	0.858	-0.131	-0.148	-0.152
	1/3	B	1.299	1.228	0.860	-0.149	-0.165	-0.170
		B'	1.300	1.229	0.860	-0.144	-0.158	-0.161
	1/2	B	1.317	1.244	0.867	-0.167	-0.188	-0.189
		B'	1.313	1.240	0.865	-0.149	-0.163	-0.168
	2/3	B	1.374	1.296	0.893	-0.201	-0.231	-0.221
		B'	1.336	1.262	0.873	-0.154	-0.169	-0.175

Table 3: F_{II,λ_2} for two diamond-shaped inclusions at the corners B and B' under in-plane shear (Plane strain state, $\nu_1 = \nu_2 = 0.3$).

In-plane shear: F_{II,λ_2}

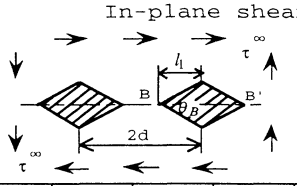

$\left(F_{II,\lambda_2} = K_{II,\lambda_2} / \tau^{\infty} \sqrt{\pi} l_1^{1-\lambda_2}\right)$

θ_B	l_1/d		G_2/G_1 10^{-5}	10^{-2}	10^{-1}	10^{1}	10^{2}	10^{5}
30°	0	B,B'	1.154	1.126	1.026	— —	— —	-0.584
	1/3	B	1.181	1.150	1.041	— —	— —	-0.611
		B'	1.172	1.142	1.035	— —	— —	-0.570
	1/2	B	1.226	1.192	1.067	— —	— —	-0.655
		B'	1.191	1.159	1.045	— —	— —	-0.567
	2/3	B	1.325	1.284	1.123	— —	— —	-0.694
		B'	1.218	1.183	1.058	— —	— —	-0.567
60°	0	B,B'	1.599	1.586	1.507	— —	-0.721	-0.651
	1/3	B	1.620	1.635	1.542	— —	-0.742	-0.685
		B'	1.626	1.612	1.525	— —	-0.717	-0.643
	1/2	B	1.743	1.724	1.606	— —	-0.759	-0.730
		B'	1.654	1.638	1.544	— —	-0.709	-0.639
	2/3	B	1.949	1.921	1.745	— —	-0.804	-0.824
		B'	1.689	1.671	1.567	— —	-0.699	-0.636
90°	0	B,B'	4.279	4.318	4.723	-0.987	-0.769	-0.769
	1/3	B	4.507	4.541	4.911	-0.967	-0.752	-0.752
		B'	4.365	4.403	4.799	-0.970	-0.753	-0.753
	1/2	B	4.944	4.967	5.260	-0.946	-0.737	-0.737
		B'	4.434	4.471	4.864	-0.954	-0.737	-0.737
	2/3	B	5.888	5.881	5.968	-0.931	-0.736	-0.736
		B'	4.504	4.541	4.931	-0.935	-0.717	-0.717

fundamental density functions and the power series. By examining the results for the various sizes, spacing and elastic parameters of inclusions, it was confirmed that the present method has good convergency of the numerical results in almost 4 digits when the number of collocation points near the corner is 12 (total number of collocation points is 96).

(2) The interaction effect of two diamond-shaped inclusions was considered. It considered the three fundamental types of loading conditions, (i) uniaxial tension, (ii) biaxial tension and (iii) in-plane shear. As a result, it was found that the interaction effect appears largely when the loading type is uniaxial tension in y-direction, $\theta_B = 90°$ and $G_2 / G_1 > 1$ (F_{I,λ_1} at the corner B increases by about 50 percent) , and when the loading type is in-plane shear, $\theta_B = 90°$ and $G_2 / G_1 < 1$ (F_{II,λ_2} at the corner B increases by about 40 percent). The interaction effect was not very large in most cases except for the two cases.

References

1. Dundurs, J. Discussion of edge-bonded dissimilar orthogonal elastic wedges under normal and shear loading, *Journal of Applied Mechanics*, 1969, **36**, 650-652.
2. Theocaris, P.S. The order of singularity at a multi-wedge corner of composite plate, *International Journal of Engineering Science*, 1974, **12**, 107-120.
3. Hattori, T., Sakata, S., Hatsuda, T. & Murakami, G. A stress singularity parameters approach for evaluating adhesive strength, *Transactions of the Japan Society of Mechanical Engineers (JSME)*, 1988, **54**-499 A, 597-603.
4. Chen, D.H. & Nisitani, H. Stress fields near the corner of jointed dissimilar materials, *Transactions of the JSME*, 1991, **57**-534 A, 366-372.
5. Chen, D.H. & Nisitani, H. Singular stress field near the corner of jointed dissimilar materials, *Journal of Applied Mechanics*, 1993, **60**, 607-613.
6. Chen, D.H. & Nisitani, H. Analysis of singular stress fields around a corner tip of inclusion, *Transactions of the JSME*, 1991, **57**-542 A, 2504-2508.
7. Chen, D.H. & Nisitani, H. Singular stress field at inclusion corner, *Modeling, Computation and Analysis in Fracture Mechanics*, ed. Y. Fujitani et al., pp. 93-113, Kinokuniya, 1994.
8. Noda, N.-A. & Matsuo, T. Singular integral equation method in the analysis of interaction between elliptical inclusions, *Transactions of the JSME*, 1994, **60**-578 A, 2411-2417.
9. Noda, N.-A., Matsuo, T. & Ishii, H. Tension of a wide plate containing a row of elliptical inclusions, *Transactions of the JSME*, 1995, **61**-581 A, 106-113.
10. Noda, N.-A., Matsuo, T., Harada, S. & Nakamura, M. Singular integral equation method in the analysis of interaction between ellipsoidal inclusions, *Transactions of the JSME*, 1995, **61**-581 A, 965-973.
11. Noda, N.-A. & Oda, K. Analysis of stress intensity factors of interface cracks and angular corners using the singular integral equation of the body force method, *Transactions of the JSME*, 1994, **60**-578 A, 2213-2219.
12. Chen, D.H. & Nisitani, H. Singular stress fields near the tip of a V-notch in a semi-infinite plate, *Transactions of the JSME*, 1991, **57**-538 A, 1406-1411.
13. Chen, D.H. & Nisitani, H. Analysis of intensity of singular stress field at fiber end (1st report, Method of analysis), *Transactions of the JSME*, 1992, **58**-554 A, 1834-1838.